HYDROTHERMAL MINERALS AND HYDROLOGIC EVOLUTION OF THE ROTOKAWA GEOTHERMAL SYSTEM, NEW ZEALAND

Mark P. Simpson[1], Amando G. Morales[2], Isabelle Chambefort[1], Samantha Alcaraz[1], Shunsuke Moribe[3], Sarah D. Milicich[4], Aimee Calibugan[5]

[1]GNS Science, Wairakei Research Centre, 114 Karetoto road, Taupō 3377, New Zealand

[2]4 Toi Grove, Turangi, 3334, New Zealand

[3]INPEX Corporation, Akasaka Biz Tower 33F, 5-3-1 Akasaka, Minato-ku, Tokyo, Japan, 107-6332

[4]GNS Science, Avalon, Lower Hutt 5010, New Zealand

[5]Mercury New Zealand Limited, 283 Vaughan Rd, Owhata, Rotorua 3010, New Zealand

m.simpson@gns.cri.nz

Keywords: *Hydrothermal minerals, hydrothermal eruptions, SWIR reflectance spectroscopy, XRD, fluid inclusions, Rotokawa.*

ABSTRACT

The Rotokawa geothermal system in the Taupō Volcanic Zone is ~28 km^2 in areal extent and has been the site of eight large hydrothermal eruptions. This study documents hydrothermal minerals for 15 wells (3,242 samples). Quartz, chlorite, albite, calcite, pyrite, and illite are the most common hydrothermal minerals. Epidote and smectite are less common. Kaolinite is uncommon. Smectite occurs as a 250 to 900 m thick carapace overlying illite and separated by a narrow intervening interval of mixed-layered illite-smectite. Chlorite is generally ubiquitous at depths ≥700 m, calcite is most common at >750 m, and epidote >1,000 m. Hydrothermal albite is present in all wells, whereas rarer adularia is patchily distributed. Chalcedony unusually occurs at >1200 m depth. Kaolinite patchily occurs at surface and locally to 200 m depth. Kaolinite further occurs up to 1,150 m depth in two wells bordering the resistivity margin. Dickite and / or kaolinite ± alunite is present in three wells (same pad) between 475 and 585 m depth.

Hydrothermal minerals correlate with fluid types. Quartz, chlorite, albite, adularia, illite, calcite and epidote coincide with alkali chloride waters. Shallow kaolinite ± sulfur coincide with acid sulfate condensates. Dickite / kaolinite ± alunite at depth are interpreted to have formed from in-situ acid sulfate condensates. Whereas deep marginal kaolinite is inferred to have formed from steam-heated CO_2-rich waters. Fluid inclusion and hydrothermal mineral inferred temperatures generally match measured temperatures, but the northern and north-eastern wells are cooler (up to 55°C to 1.5 km depth). A 3-stage hydrologic model is proposed relative to hydrothermal eruptions that occurred between ~20,000 and 3500 years ago. 1) Pre-eruption, with hotter and greater fluid flow to the north. 2) Syn-eruptions with creation of greater permeability in the south. Associated decompressive boiling resulted in chalcedony deposition at depth. Local transient temperature changes resulted in pressure draw down and formation of anhydrite (to 500 m depth). 3) Post-eruptions to present day with enhanced permeability in the south. Greater fluid and heat transfer in the south coupled with reduced fluid and heat transfer elsewhere has resulted in cooler conditions in the north to <1.5 km depth.

1. INTRODUCTION

Geothermal systems provide a unique environment where the interaction of thermal fluids with the host rocks generate hydrothermal minerals that can be correlated with measured temperatures, permeability and fluid type (Steiner, 1977; Browne 1978; Reyes, 1990; Simmons and Browne, 2000). In this study, we document hydrothermal minerals in drill cuttings from 15 wells from the Rotokawa geothermal system (Fig. 1). Some 3,242 samples have been analysed by stereo-microscope examination, acid and magnetic testing, and short-wave infrared (SWIR) reflectance spectroscopy. Clay separate X-ray diffraction (XRD) analyses were made on 359 samples. Temporal mineral relationships were resolved from thin section and scanning electron microscopy. Fluid inclusions have also been measured to determine fluid temperatures. Combined, these reveal system scale zonation of hydrothermal minerals and temperature conditions. These have been compared against the currently understood thermal, hydrologic and fluid compositional structure of the present-day Rotokawa geothermal system and reveal some changes with time.

2. ROTOKAWA GEOTHERMAL SYSTEM

Surficial thermal features and areas of altered ground at Rotokawa cover ~2.5 km^2 and occur within a 28 km^2 resistivity geophysical anomaly (Fig. 1) outlining the <1,000 m depth extent of hot water and clay alteration (Risk, 2000). Thermal features are concentrated in two areas (Krupp et al., 1986; Browne, 1989). Most occur in the southern area and the main feature is the acidic Lake Rotokawa. An extensive area of steaming ground with fumaroles, acid sulfate-chloride springs, and dissolution craters occurs NE of the lake. In the northern area there are fewer thermal features with dilute chloride-CO_2 springs along the Waikato River and local steaming ground near RK8 (Fig. 1). Former steaming ground occurs near RK6 (Browne, 1989). Breccia deposits from eight large hydrothermal eruptions cover ~15 km^2 (Fig. 1) and are collectively known as Parariki breccia (Collar and Browne, 1985). The breccias are between ~20,000 and 3550 years with most <6060 years. Five vent centres are recognised extending over 1.7 km and broadly aligned towards the NE. Lake Rotokawa is the site of two hydrothermal eruptions. Rhyolite ejecta from one eruption is identical to Oruahineawe Formation rhyolite in a proximal well suggesting it was sourced from ~450 m depth (Collar and Browne, 1985).

The Rotokawa geothermal system is hosted in rhyolitic pyroclastic, rhyolite lavas, intercalated sedimentary rocks, plus andesite lavas and breccias (Fig. 2). These unconformably overlie greywacke basement intersected in the southern wells (Milicich et al., 2020; and references therein). Three major NE–SW striking normal faults have been determined from stratigraphic correlations and offset the greywacke and andesite. The NW dipping Central Field Fault, possibly comprised of several faults and associated damage zones has >800 m vertical displacement (Wallis et al., 2003; Milicich et al., 2020).

ISSN 2703-4275

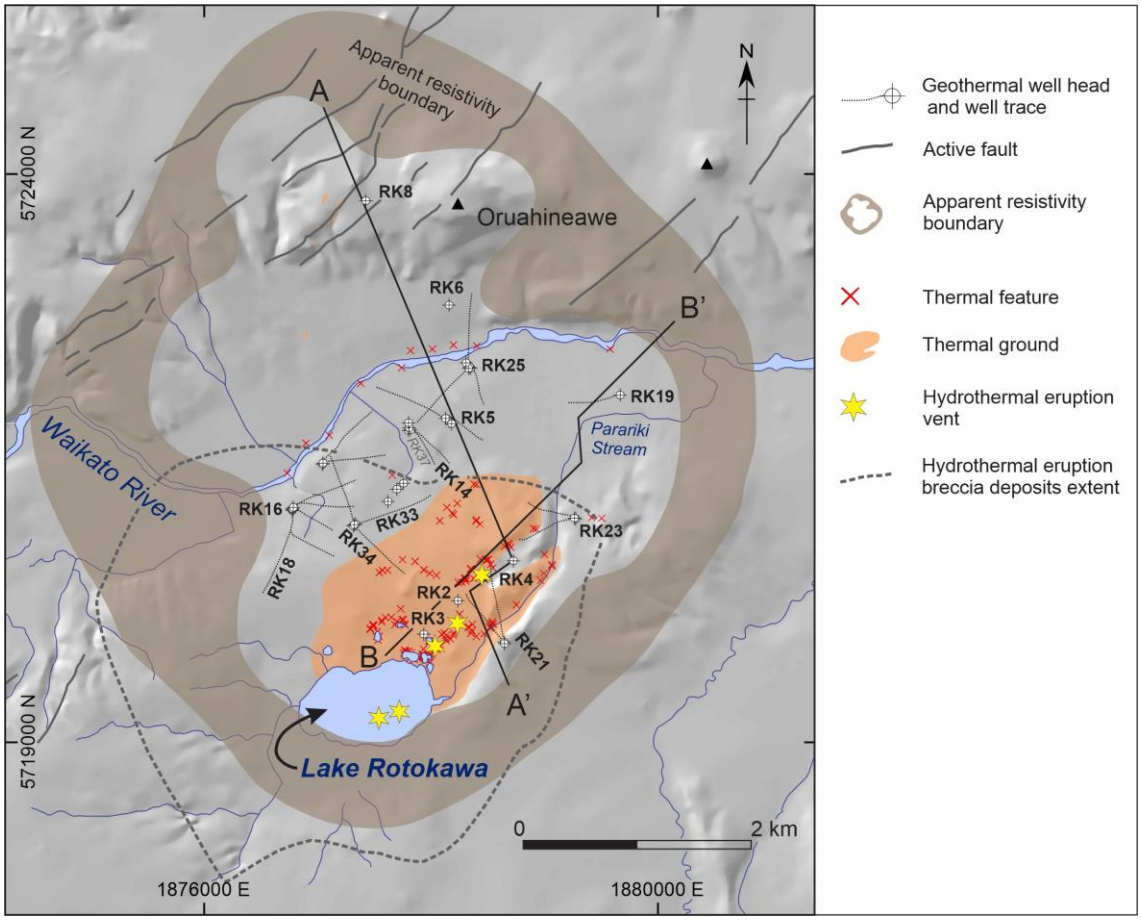

Figure 1: Hill shaded topographic map of the Rotokawa area showing thermal features, eruption centres (Collar and Browne 1985), wells, and resistivity anomaly (Risk, 2000).

The hydrologic and chemical structure of the geothermal system is complex and broadly comprised of 1) A deep (>0.8 km), hot (300° to 340°C) liquid-dominated chloride (850–450 ppm) reservoir with hotter temperatures in the south (up to 337°C) and cooler to the north (up to 310°C) (Hedenquist et al., 1988; Winick et al., 2011). 2) An intermediate aquifer with mixed combinations of boiled chloride waters, gas-rich steam condensates (CO_2 / H_2S), acid sulfate-chloride and heated ground water. 3) A shallow aquifer with steam-heated, acid sulfate (variable chloride content) and chloride-CO_2 waters. Conceptually, the reservoir is fed by an upflow zone in the south (Winick et al., 2011). The fluid rises and boils with deep outflow towards the north and is diluted by deep marginal fluids and modified via fluid:rock interactions resulting in temperature and chemical gradients. The Central Field Fault provides a zone of focused upflow and enhanced vertical permeability, establishing a two-phase (boiling) region throughout much of the deep reservoir and into the intermediate aquifer (Winick et al., 2011; Sewell et al., 2015).

3. HYDROTHERMAL MINERALS AND ALTERATION

Hydrothermal mineral occurrences have been documented for 15 wells for 3,242 samples that are on average spaced 10 m apart. The intensity of alteration ranges from weak (<25%) to strong (>75% altered). Most volcanic rocks are moderate to strongly altered (~65 to 85%) with variable amounts of persistent magnetite and plagioclase. Magnetite abundance is useful in assessing the degree of alteration for Rotokawa Andesite. Andesite in the northern most well RK8 has the least occurrences and amount of magnetite (Fig. 2). RK6 (1.1 km to SE) has low amounts of magnetite, as does RK25 and RK16. By contrast, andesite in southern wells in the footwall of the Central Field Fault (RK4, RK19, RK21, and RK23), has the most magnetite and is less altered compared to andesite elsewhere. In the following, depth measurements specified refer to vertical depth below the current ground surface.

The rocks are altered to a variety of hydrothermal minerals, some of which have also been deposited in cavities and veins. Common hydrothermal minerals include quartz, chlorite, albite, calcite, pyrite, illite (in >45% of samples), and less common epidote, smectite and adularia (in 20 to 40% of samples). Mixed-layered illite-smectite, cristobalite, mordenite and kaolinite are uncommon (5 to 15% of samples). Chalcedony, siderite, anhydrite, dickite, alunite, wairakite, actinolite, biotite and buddingtonite are rare (<2% of samples). The occurrence, spatial distribution and temporal relationships of selected minerals are described below. Mineral distributions have been evaluated in 3D using Leapfrog and their occurrences presented here on two cross sections (Figs. 3 & 4).

Quartz, Chalcedony and Cristobalite: Quartz is a ubiquitous hydrothermal mineral present in weak to strongly altered rocks throughout the drilled extent of the geothermal system. It predominately occurs as a very fine-grained alteration mineral of the volcanic rock matrix. Quartz has also been deposited in cavities and veins (<2 mm wide). Quartz pseudomorphs of chalcedony are

ISSN 2703-4275

present in ~4% of samples and mostly occurs in cavities and veins hosted in Rotokawa Andesite. It is seen in most wells at depths of 1200 to 2900 m below ground surface but is absent in RK8 and RK5 (Figs. 3 & 4). In thin section, chalcedony is recrystallised to quartz. Chalcedony can predate or postdate deposition of chlorite, epidote and calcite. In addition, rare cavities can have spherical quartz after opal. Cristobalite identified in clay separate XRD scans is present in shallow samples to a depth of 700 m. It is most common in RK16, RK19 and RK25.

Chlorite: This clay is the second most common hydrothermal mineral in 72% of samples. It is generally ubiquitous at depths ≥700 m (Figs. 3 & 4) but can occur at shallow depths of ≥150 m in some wells (e.g. RK3, RK4, RK14). Petrography reveals chlorite is a significant alteration mineral in the matrix of volcanic rocks. This is especially the case for Rotokawa Andesite where chlorite can be volumetrically more abundant than quartz. Chlorite pseudomorphs both pyroxene and amphibole, plus further fills cavities and fractures (<0.5 mm wide). Chlorite is the dominant mineral filling cavities in Rotokawa Andesite overgrowing quartz and epidote.

Chlorite composition has been spectrally approximated from the Fe-OH wavelength position. The hull quotient corrected Fe-OH wavelength values for chlorite in volcanic rocks shows considerable variation (Fig. 5) although intervals with consistent values (2250 to 2255 nm) mainly seen for andesite correspond to an Fe-Mg chlorite (Pontual et al., 1997). Most chlorite in greywacke is Mg-rich (2242 to 2244 nm) and metamorphic, although there is some Fe-Mg chlorite (2248 to 2256 nm) attributed as hydrothermal (Fig. 5).

Illite, Mixed-layered illite-smectite and Smectite: These clays have been identified from clay separate XRD (n=359) and broadly from SWIR spectroscopy (n=3,242). Spectral differentiation is based on the H_2O/Al-OH depth ratio, but these features can be shared by other minerals affecting the value (Simpson and Rae, 2018). Smectite can be spectrally masked by volcanic glass, opal, and kaolinite. Thus, the boundaries between illite, illite-smectite and smectite are based on XRD, although illite is accurately outlined from spectroscopy (Figs. 3, 4 & 5). Widespread smectite forms a carapace that can extend 250 to 900 m below surface (Figs. 3 & 4).

An extensive zone of illite occurs below the smectite with shallow occurrences in RK2 and RK3, and a shallow NE extending tongue in RK5 and RK14. Between smectite and illite in most wells is an intervening interval of missed-layered illite-smectite with 50 to 95% illite interlayering and a maximum vertical extent of ~300 m. Thin section examination and spectral response indicate illite occurs in volumetrically variable amounts that are commonly low.

The composition of illite has been broadly approximated from spectral analysis (Fig. 5). Illite in volcanic rocks with a hull corrected Al-OH wavelength value of between 2195 and 2212 nm is muscovitic [$KAl_2(AlSi_3O_{10})(OH)_2$] (Pontual et al., 1997). Illite in greywacke with higher Al-OH wavelength values between 2215 and 2230 nm is aluminoceladonitic [$K(Mg,Fe^{2+})Al(Si_4O_{10})(OH)_2$] and metamorphic. Some illite in greywacke is muscovitic and presumed hydrothermal.

Hydrothermal Albite and Adularia: Based on XRD (n=187), hydrothermal albite is more common than adularia (76% versus 33%). Albite is present in all wells studied at >300 m depth, whereas adularia is in general patchily distributed (Figs. 3 & 4). Adularia is most vertically continuous in RK4 and RK5. Albite and adularia both replace plagioclase. Plagioclase can be incipient to completely altered by 'dusty' microscopic inclusion-rich albite together with or without one or more of the following minerals including epidote, calcite, illite, adularia and chlorite. Epidote appears contemporaneous with albite, whereas illite and calcite appear later stage. Adularia typically is a minor alteration mineral of plagioclase occurring within or adjacent internal micro-fractures.

Epidote: Epidote visually recognised in 24% of cuttings is typically present in trace amounts (<0.5 vol.%). Epidote occurs in most wells at depths >1050 m (Figs. 3 & 4) but is rare in RK4 and absent in RK19 and RK23. Wells RK21, RK25 and RK33 have intervals with 1 to 5 vol.% epidote (Fig. 3). Epidote is an alteration mineral of plagioclase, pyroxene, and amphibole. Epidote also fills cavities and veins (≤2 mm wide) that are most common in Rotokawa Andesite. Epidote veins are typically monomineralic with up to three generations recognised. In cavities, epidote can be overgrown by chlorite, chalcedony or calcite, but less commonly can overgrow these minerals. Drill core examination reveals epidote can be common in half the core but in the other half minor to absent with instead common calcite.

Calcite and Siderite: Calcite is the third most common hydrothermal mineral present in 69% of samples. Calcite can occur at shallow depth typically in trace amounts (<0.5%), but generally is most common and in greater abundance (1 to 15%) at depths ≥750 m (Figs. 3 & 4). Calcite is an alteration mineral of plagioclase. Where plagioclase is altered to albite with or without epidote, adularia or illite; calcite overprints these minerals. Calcite fills veins up to 6 mm wide; most are monomineralic and cut earlier quartz and epidote veins. In cavities, calcite commonly overgrows chlorite, chalcedony, and epidote, but rarely it can precede these minerals. Veins of platy calcite are rare (0.7% samples), and most frequent in RK19. Platy calcite occurs from 300 m to greater than 3050 m depth, with the bladed morphology indicating formation from a boiling fluid (Tulloch, 1982). Siderite is rare (2.1% of cuttings) and mainly occurs as an open space deposited mineral coating fractures. It is found in RK19 and RK23 between ~400 and 850 m depth (Fig. 4).

Mordenite and Wairakite: Mordenite, identified in 8% of clay XRD scans occurs from near surface to 500 m deep overlapping with smectite (Figs. 3 & 4). Mordenite could be more common, but its known occurrence limited due to detection technique. Rare wairakite was identified in thin section with the shallowest and deepest occurrences ~1100 m and 2850 m, respectively.

Pyrite and Pyrrhotite: Pyrite is present in 61% of cuttings and in rocks from all depths. It is essentially ubiquitous in some wells but in others there can be significant intervals without pyrite (e.g. RK23). Pyrrhotite in 0.2% of samples is mostly found in RK21 and RK23 as pseudohexagonal crystals deposited in open spaces.

ISSN 2703-4275

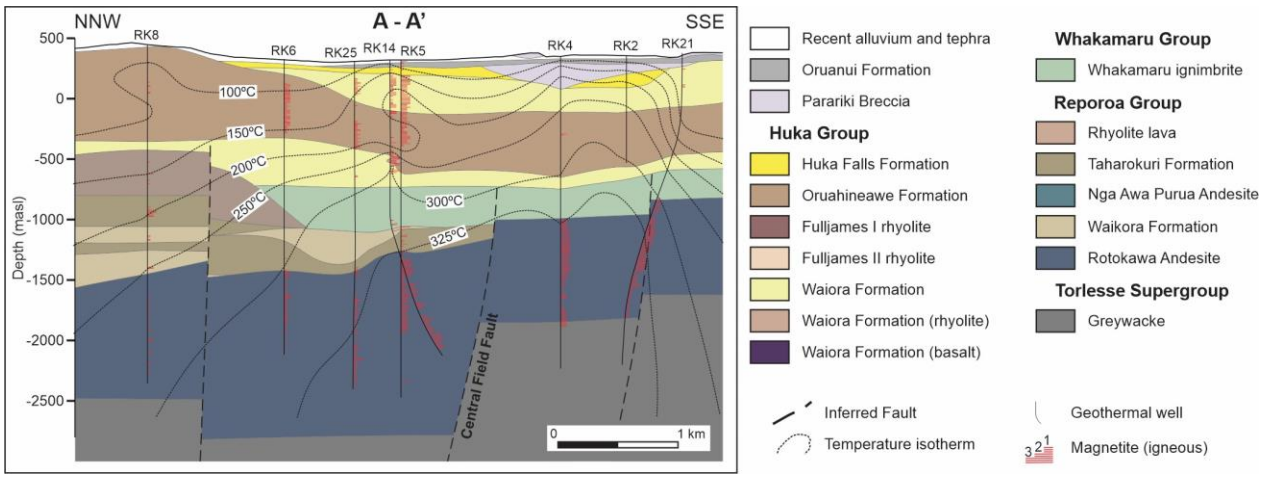

Figure 2: Geology cross section of the Rotokawa geothermal system (Milicich et al., 2020) with temperature isotherms (Mercury Ltd.) and the semi-quantitative amount of igneous magnetite. Location of cross section shown in Figure 1.

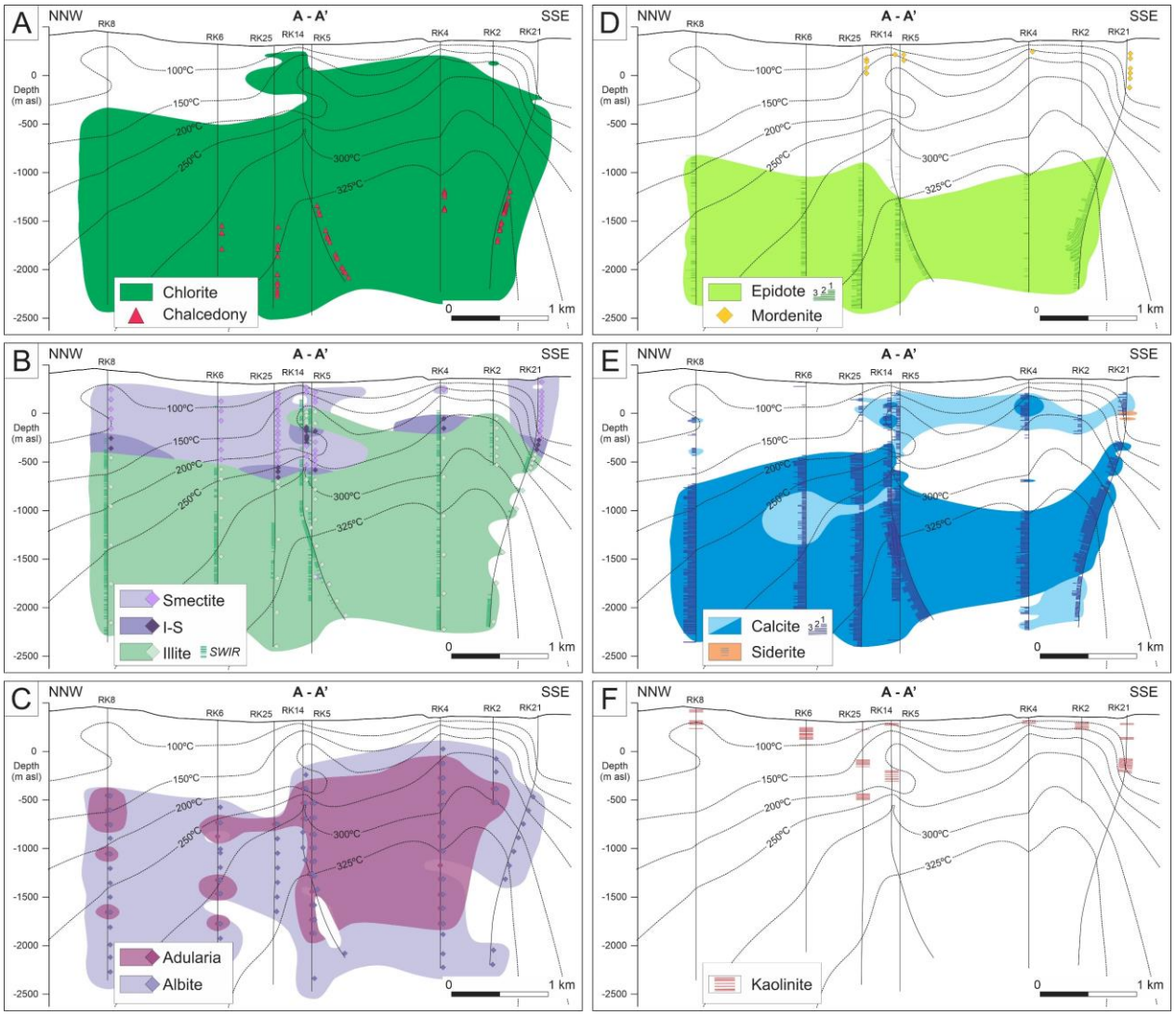

Figure 3: NNW-SSE cross section showing hydrothermal mineral distributions. A) Chlorite (SWIR & XRD) plus chalcedony (visual). B) Illite, illite-smectite, and smectite (XRD = diamond symbols & SWIR illite = dash). C) Albite and adularia (XRD). D) Epidote (visual) plus mordenite (XRD). Amount of epidote approximated (0.5%, 0.5–1%, >2%). E) Calcite and siderite. Amount of calcite approximated from acid testing (<0.5%, 1–10%, >10%). F) Kaolinite (SWIR). Location of cross section shown in Figure 1.

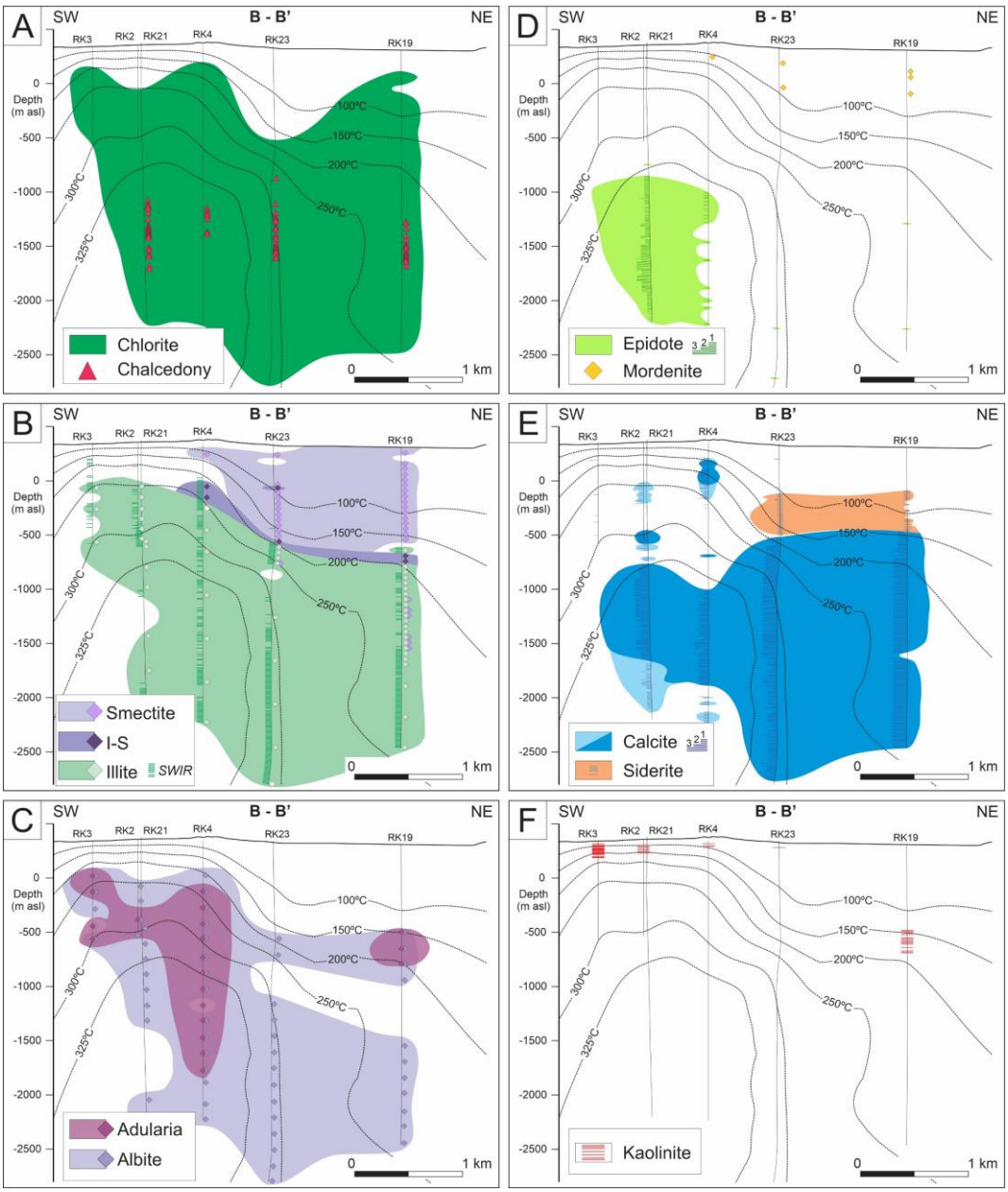

Figure 4: SW-NE cross showing hydrothermal mineral distributions. A) Chlorite (SWIR & XRD) plus chalcedony (visual). B) Illite, illite-smectite, and smectite (XRD = diamond symbols & SWIR illite = dash). C) Albite and adularia (XRD). D) Epidote (visual) plus mordenite (XRD). Amount of epidote approximated (0.5%, 0.5–1%, >2%). E) Calcite and siderite. Amount of calcite approximated from acid testing (<0.5%, 1–10%, >10%). F) Kaolinite (SWIR). Location of the cross sections are shown in Figure 1.

Kaolinite, Dickite and Alunite: These minerals have been identified from SWIR spectroscopy and XRD. Kaolinite and alunite have previously been reported as common in surface rocks (Krupp et al., 1986) and as a common alteration and vein mineral in the clasts and matrix of surface exposed Pararíki breccia (Collar and Browne, 1985). Since no cuttings are available from the conductor casing (to 30 m), we do not know the extent of kaolinite and alunite over this interval.

Kaolinite from this study is present in ~5% of cuttings occurring patchily near surface and is most common in RK3, RK6 and RK8 to ~200 m depth (Fig. 3 & 4). There are local deeper occurrences of kaolinite with the deepest in RK18 (~950–1150 m) and RK19 (~800–1000 m) located towards the western and eastern resistivity boundary, respectively. Dickite is rare and present in RK14 together with ± kaolinite and ± alunite at a depth of 475 to 585 m. Dickite has also been identified in RK9 and RK37 (same drill pad as RK14) over an identical depth interval. Alunite is rare with most in RK14 and RK37 at a depth of 495 to 560 m. Elsewhere, alunite has only been spectrally detected in four shallow samples in RK2, RK3, and RK8 (30 to 160 m).

Anhydrite: Uncommon anhydrite is visually identified as a cavity and vein fill in RK2 and RK3 between 230 to 470 m and 365 to 535 m, respectively. Anhydrite also occurs sporadically at >1750 m depth in wells RK5, RK24, RK27 and RK30 as both an alteration mineral and in veins overgrown by calcite (Chambefort, 2020).

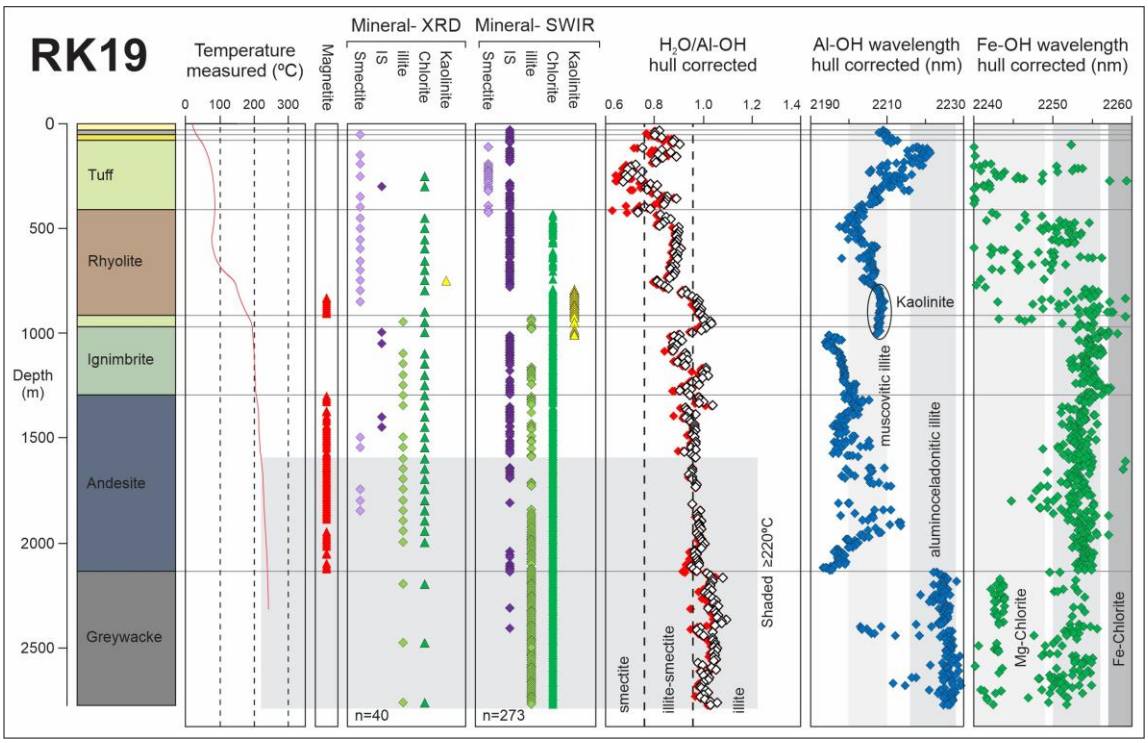

Figure 5: SWIR mineral identifications and spectral parameter plots compared against rock type, measured temperature, and clay separate XRD mineralogy for RK19. Geology is simplified and unit colour matches formations in Figure 2. Illite and chlorite in greywacke is compositionally different from that in altered volcanic rocks.

4. FLUID INCLUSIONS

Fluid inclusion homogenisation temperatures (T_h) from this and previous studies were made on two-phase liquid-rich inclusions hosted in platy calcite, calcite, quartz, anhydrite and igneous quartz (Table 1). Results are reported for individual fluid inclusion assemblages (FIA's), which is a group of inclusions trapped during a single petrographically distinguished event and confirmed following measurement by corresponding narrow T_h ranges (by analogy <10°C for epithermal; Fall and Bodnar, 2018). The T_h range for FIA's are typically narrow (2° to 14°C), however the apparent wider ranges for some are skewed by one or two spurious values due to the inadvertent measurement of modified inclusions. The relative timing of different FIA's could not be established since the groups are either spatially separated within or occur in separate crystals. However, for rare samples both primary and secondary inclusion have been measured and were trapped at different times.

Many FIA have T_h values that match or are within ±15°C of the measured temperature (Table 1). Four samples have T_h values lower than the measured (Δ >15°C) and interpreted to indicate subsequent heating following inclusion entrapment (e.g. RK33 & RK37). Conversely, there are six samples where fluid inclusion T_h values are hotter than the measured (Δ >15°C) and indicate cooling subsequent entrapment. Cooling of 30° to 55°C is noted for wells RK6, RK8, RK19, and is supported by mineral inferred temperatures that are discordant with measured temperatures (discussed below).

5. DISCUSSION

In this section we examine the relationship between hydrothermal minerals with the present-day modelled temperature, fluid composition and hydrologic structure of the Rotokawa geothermal system. Combined with fluid inclusion temperature insights, a model for the geothermal system hydrologic evolution is presented.

Measured fluid temperature and mineral geothermometry

Measured temperature ranges over which hydrothermal minerals occur at Rotokawa are shown in Figure 6. Mordenite coincides with measured temperatures of <160ºC, and cristobalite <180ºC. Most smectite aligns with temperatures of <150ºC and most illite >220ºC (Figs. 3 & 4). However, in RK8 and RK19, illite coincides with measured temperatures as low as 100ºC but formed at hotter conditions as supported from fluid inclusion measurements. All epidote, apart from that in RK8, occurs beneath the 250°C isotherm with some 94% coinciding with temperatures ≥300°C (Figs. 3 & 4). Some epidote in RK8 coincides with measured temperatures as low as 190ºC but formed under hotter conditions as supported from fluid inclusion measurements. Most kaolinite overlaps with measured temperatures of <220°C, except for in RK14 where kaolinite and dickite coincide with temperatures of 245º to 257ºC. Here kaolinite may have formed at hotter temperatures than generally accepted. Nonetheless, temperature ranges over which hydrothermal mineral occur at Rotokawa overall match those established for other geothermal systems in New Zealand and globally (e.g. Browne and Ellis, 1970; Steiner, 1977; Reyes, 1990).

ISSN 2703-4275

Table 1. Summary fluid inclusion data for Rotokawa compared against measured well temperatures.

Sample	Mineral	Type	FIA	T_h range	n	Ave.	Med.	T_m range	n	Ave.	Med.	Salinity*	T well	ΔT**	Reference
RK4 1630 mRF	Calcite	P	FIA_1	298 to 332	6	321	323	-0.7 to -2.2	6	-1.6	-1.8	1.2 to 3.7	332	-12	Rae et al. (2012)
RK5 2003 mRF	Calcite	S	FIA_1	322 to 325	6	324	324	-0.8 to -1.0	6	-0.9	-1.0	1.4 to 1.7	328	-5	This study
		S	FIA_2	332 to 335	4	333	333	-0.6 to -0.8	4	-0.7	-0.8	1.1 to 1.4		+5	
		S	FIA_3	324 to 325	3	325	325	-0.8	1	-0.8	-0.8	1.4		-3	
RK6 1175 mRF	Igneous quartz	S	FIA_1	238 to 244	5	242	242	-0.4	5	-0.4	-0.4	0.7	275	-33	Prol-Ledesma (1985)
		S	FIA_2	251 to 265	5	257	258	-0.2	1	-0.2	-0.2	0.4		-18	
		S	FIA_3	316 to 325	5	320	320	-0.3	2	-0.3	-0.3	0.5		+45	
RK8 1360 mRF	Platy calcite	P	FIA_1	256 to 257	8	256	257	-0.5 to -0.7	8	-0.6	-0.6	1.0	203	+53	This study
RK18 L2 2219 mRF	Platy calcite	P	FIA_1	320 to 330	8	327	328	-0.3 to -0.8	8	-0.5	-0.5	0.5 to 1.4	325	+3	Well report
RK19 1350 mRF	Platy calcite	P	FIA_1	252 to 254	10	253	254	-0.9 to -1.0	9	-1.0	-1.0	1.6 to 1.7	210	+43	This study
RK19 2055 mRF	Platy calcite	P	FIA_1	251 to 253	9	252	252	-0.5 to -0.6	6	-0.6	-0.6	0.9 to 1.0	235	+17	This study
RK25 2200 mRF	Calcite	P	FIA_1	335 to 342	3	337	336	-1.8	3	-1.8	-1.8	3.1	322	+15	Rae et al. (2012)
		S	FIA_2	285 to 336	8	324	330	-0.9 to -1.8	8	-1.2	-1.0	1.6 to 3.1		+2	
		S	FIA_3	329 to 332	3	331	331	-0.9 to -1.0	3	-1.0	-1.0	1.6 to 1.7		+9	
		S	FIA_4	326 to 338	7	333	333	-1.0 to -1.7	7	-1.5	-1.6	1.7 to 2.9		+11	
RK27 1854 mRF	Anhydrite	P	FIA_1	323 to 328	13	325	325	-0.1 to -0.9	13	-0.6	-0.6	0.2 to 1.6	312	+13	Rae et al. (2012)
		P	FIA_2	305 to 325	13	319	320	-0.1 to -0.7	13	-0.4	-0.5	0.2 to 1.2		+7	
		S	FIA_3	324 to 327	3	326	327	-0.1	3	-0.1	-0.1	0.2		+14	
RK27 1853 mRF	Platy calcite A	S	FIA_1	312 to 334	10	323	321	-2.0 to -2.3	5	-2.1	-2.1	3.4 to 3.9	312	+11	This study
		S	FIA_2	317 to 325	3	322	324	-	0					+10	
	Platy calcite B	S	FIA_1	322 to 333	9	328	328	-1.0 to -1.8	7	-1.3	-1.2	1.7 to 3.1	312	+16	This study
RK28 2312 mRF	Platy calcite	S	FIA_1	306 to 311	14	308	308	-0.4 to -0.9	12	-0.7	-0.8	0.7 to 1.6	314	-6	This study
		S	FIA_2	307 to 309	3	308	307	-	0					-6	
RK33 985 mRF	Platy calcite	P	FIA_2	271 to 276	4	273	272	-0.3 to -1.1	6	-0.9	-1.0	0.5 to 1.9	301	-29	Well report
RK33 1040 mRF	Platy calcite	P	FIA_1	281 to 286	4	283	282	-0.5 to -0.7	4	-0.6	-0.6	0.8 to 1.2	304	-21	Well report
RK33 2045 mRF	Platy calcite	S	FIA_1	333 to 334	4	334	334	-0.4 to -0.5	4	-0.5	-0.5	0.7 to 0.9	320	+14	Well report
		S	FIA_2	333 to 336	5	335	336	-0.9 to -1.0	5	-0.9	-0.9	1.6 to 1.7		+15	
RK34 ST-1 845 mRF	Quartz	S	FIA_1	279 to 290	18	286	288	-0.2 to -0.4	17	-0.3	-0.3	0.4 to 0.7	289	-3	Well report
RK34 ST-1 1400 mRF	Quartz	P	FIA_1	327 to 333	8	330	330	-1.5	1	-1.5	-1.5	2.6	312	+18	Well report
		S	FIA_2	297 to 309	13	304	304	-1.3 to -2.3	7	-1.8	-1.6	2.2 to 3.9		-8	
RK37 600 mRF	Platy calcite	P	FIA_1	257 to 258	11	258	258	-0.2 to -0.4	11	-0.3	-0.3	0.4 to 0.7	245	+13	Well report
RK37 1220 mRF	Platy calcite	P?	FIA_1	249 to 280	17	268	273	0 to -0.5	14	-0.2	0.0	0 to 0.9	305	-37	Well report

All temperatures °C. P = primary, S = Secondary. FIA # denotes group and not formation sequence.
T well = measured well temperature at sample depth (Mercury Ltd data).
** ΔT = FIA T_h average - measured temperature; + value = T_h > measured, – value = T_h < measured.

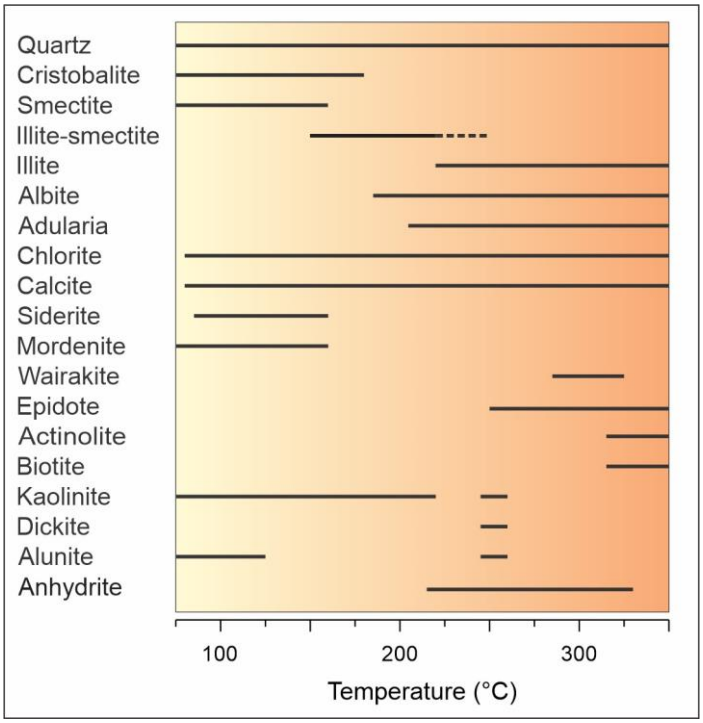

Figure 6: Measured temperature ranges over which hydrothermal minerals occur at the Rotokawa geothermal system.

ISSN 2703-4275

Thermal change

Comparison of mineral inferred, fluid inclusion and present-day measured temperatures reveal thermal change that is unrelated to field development. Past hotter temperatures are noted in wells RK8, RK6 and RK19 that occur towards the north and northeastern resistivity boundary (Fig. 1). Temperatures were up to 50°C (illite & epidote inferred) to 55°C (fluid inclusion at 1360 m) hotter in RK8 and 45°C hotter in RK6 (fluid inclusion at 1175 m). Temperatures in RK19 were 30°C (illite inferred) to ~45°C (fluid inclusion) hotter than present. Fluid inclusions from RK19 further reveal this temperature difference is less with depth (ΔT of 43°C at 1350 m and 17°C at 2055 m; Table 1).

Acid sulfate condensates

Kaolinite with some sulfur at and near surface (<200 m) have formed from acid sulfate condensates that originate in the vadose zone via oxidation of H_2S exsolved from boiling chloride waters. Deep occurring kaolinite and / or dickite ± alunite in RK9, RK14 (and RK37) has formed from in-situ former acid sulfate condensates as proposed by Bowyer et al. (2008). Given the lateral (≥75 m) and vertical (~100 m) extent of these acid minerals coupled with calcite alteration above and below this zone, it is improbable they formed from a descending acid fluid.

Decompression

Chalcedony generally forms at temperatures of <180°C (Fournier, 1985), but quartz after chalcedony and opal at depth in Rotokawa Andesite mostly coincides with measured temperatures of >300ºC (Figs. 3 & 4). While some chalcedony could have formed at <180ºC during system inception, most overgrows other hydrothermal minerals including epidote inferred to form at >250°C. For chalcedony or opal to precipitate at high temperatures the fluid must become oversaturated with respect to silica, which is possible by sharp decompression resulting in boiling and cooling (Fournier, 1985). Chalcedony at Bulalo Philippines is attributed to catastrophic decompression and boiling (Stimac et al., 2006). The widespread occurrence of chalcedony at Rotokawa, except in RK8 & RK5, suggests decompression over much of the system. Temporal mineral relationships with chalcedony deposited at different times relative to other minerals infers that there have been several depressurisation events. These are likely related to the multiple large hydrothermal eruptions (Price et al., 2011).

Hydrologic evolution of the Rotokawa geothermal system

Hydrothermal minerals, their inferred formation temperature and associated fluid composition are generally conformable to the currently understood thermal, chemical and hydrologic structure of the Rotokawa geothermal system. However, there are divergencies indicative of past change. A 3-stage hydrologic model is proposed pre-, syn- and post- Parariki breccia (~20,000–3550 year) hydrothermal eruptions.

1) Pre-hydrothermal eruptions. Thermal activity in the past was more significant in the northern portion of the geothermal system than present. Current surface thermal activity north of the Waikato River is limited but areas of altered ground, now cold, indicate former more widespread thermal activity (Browne, 1989). In the wells towards the north and northeast system margins inferred by resistivity, relict epidote (RK8) and illite (RK8 and RK19), coupled with fluid inclusion results (RK6, RK8, and RK19), indicate former hotter subsurface conditions (up to 55°C to 1.5 km depth). The andesite in RK8 and to a lesser extent in RK6 has notably less magnetite compared to andesite elsewhere (Fig. 2) and generally is more highly altered. Coupled, these data indicate past hotter temperatures and infer greater water-rock interactions with chloride waters in the north.

2) Syn-eruptions. There have been at least eight significant hydrothermal eruptions in the southern portion of the geothermal field that broadly align with the Central Field Fault. Most eruptions have occurred over a narrow time frame of ~2500 years (n=6 between 6060 and 3550 years; Montanaro, personal communication 2021) and occur within a broad topographic depression now partly occupied by Lake Rotokawa and Parariki Stream the only outlet. The initial hydrothermal eruption likely involved magmatic gas (CO_2) and heat. Some subsequent hydrothermal eruptions partly primed by reduced magmatic gas and partial mineral sealing (quartz and alunite; Collar and Browne, 1985) could have been triggered by repeated filling and drainage of a paleo-lake filling the broad depression. Irrespective of the cause, decompression associated with the hydrothermal eruptions is considered responsible for chalcedony and opal deposition at depth on multiple occasions. More significantly, each eruption enhanced permeability with fracture zones and possibly the eruption vent permitting increased fluid discharge to the surface effecting both temperature and pressure. Enhanced channeled fluid flow can result in isotherm contraction towards the permeable zone due to increased convective heat loss and coupled pressure reduction. Localised transient pressure reduction likely resulted in acid sulfate fluid drawdown forming anhydrite (0.2 to 0.5 km) and some kaolinite (to 0.2 km depth); the former precipitated on contact with hotter rock due to its inverse solubility.

3) Post-hydrothermal eruption to present. Based on present-day fluid chemistry and temperature gradients the main upflow of chloride waters occurs in the south with deep outflow towards the north (Winick et al., 2009). Fracturing adjacent and beneath multiple hydrothermal eruption vents and concomitant small-scale opening of the Central Field Fault and / or associated damage zones has overall resulted in increased permeability in the south. At a system scale and over time, greater flow and higher heat transfer in the south has resulted in reduced fluid flow and heat transfer further afield. Reduced fluid and heat flux towards the north (RK8) and northeast (RK6 and RK19) is proposed to have resulted in cooling by up to 55°C to a depth of 1.5 km. However, temperatures in RK8 are still hot (280°C at 2.4 km). Localised kaolinite ± dickite, ± alunite at depth in RK9, RK14 and RK37 presumably has formed post-eruption from in-situ acid sulfate condensate. Whereas, deeper marginal kaolinite in RK18 and RK19 has formed from CO_2-rich steam heated waters. The present hydrological structure of the shallow and intermediate aquifer between chloride, steam-heated and heated groundwater is complex and could still be adjusting to the effects of multiple hydrothermal eruptions.

ISSN 2703-4275

6. CONCLUSION

The Rotokawa geothermal system has a complex hydrology and from hydrothermal minerals, a complex geothermal history. Temperatures have reduced towards the north and along the north eastern resistivity boundary due to inferred changing fluid focus, heat flux and pressure gradients. This has occurred in response to enhanced permeability centred in the south that is spatially linked with large hydrothermal eruptions. These eruptions have impacted the hydrological and thermal structure of the geothermal system at different physical and time scales.

ACKNOWLEDGEMENTS

We thank Mercury NZ Ltd and the Rotokawa Joint Venture for access to rocks and field data. Funding was provided from GNS Sciences (C05X1702: Strategic Science Investment Fund, New Zealand's Geothermal Future). Shannen Mills and Shane Cronin are thanked for feldspar XRD scans. Peter Johnson is thanked for insightful discussion on fluid flow modelling. Breccia discussions with Shane Cronin and Cristian Montanaro have been illuminating and thought provoking.

REFERENCES

Bowyer, D., Bignall, G., and Hunt, T.: Formation and neutralisation of corrosive fluids in the shallow injection aquifer, Rotokawa Geothermal Field, New Zealand. Geothermal Resource Transactions (2008).

Browne, P.R.L.: Hydrothermal alteration in active geothermal fields: Annual review of Earth and Planetary Science 6, pp. 229–250 (1978).

Browne, P.R.L.: Investigations at the Rotokawa Geothermal Field, Taupo Volcanic Zone, New Zealand. Journal Geothermal Resource Society Japan 11, pp. 87–96 (1989).

Browne, P.R.L. and Ellis, A.J.: The Ohaki-Broadlands geothermal area, New Zealand: mineralogy and related geochemistry. American Journal of Science 269, pp. 97–131 (1970).

Chambefort, I.: Sulfur in New Zealand geothermal systems: insights from stable isotope and trace element analyses of anhydrite from Rotokawa and Ngatamariki geothermal fields, Taupo Volcanic Zone. New Zealand Journal of Geology and Geophysics XXX, pp. 372–388 (2000).

Collar, R.J., and Browne, P.R.L.: Hydrothermal eruptions at the Rotokawa Geothermal Field, Taupo Volcanic Zone. Proc. 7th New Zealand Geothermal Workshop, Auckland, New Zealand (1985).

Fall, A., and Bodnar, R.J.: How precisely can the temperature of a fluid event be constrained using fluid inclusions? Economic Geology 113, 1817–1843 (2018).

Fournier, R.O.: "The behavior of silica in hydrothermal solutions." Geology and Geochemistry of Epithermal Systems: In Berger, B.R., and Bethke, P.M., eds. Reviews in Economic Geology (1985) 2, pp. 45–62.

Hedenquist, J.W., Mroczek, E.K., and Giggenbach, W.F.: Geochemistry of the Rotokawa geothermal system: Summary of data, interpretation and appraisal for energy development, Chemistry Division DSIR Technical Note, 88/6 (1988).

Krupp, R., Browne, P.R.L. Henley, R.W., and Seward, T.M., Rotokawa Geothermal Field. Berlin-Stuttgart, Gerbruder Borntrager, Monograph Series Mineral Deposits 26, pp. 47–55 (1986).

Milicich, S.D., Chambefort, I., Wilson, C.J.N., Alcaraz, S., Ireland, T.R., Bardsley, C., and Simpson, M.P.: A zircon U-Pb geochronology for the Rotokawa geothermal system, New Zealand, with implications for TVZ evolution. Journal of Volcanology & Geothermal Research 389, Article 106729 (2020).

Pontual, S., Merry, N., and Gamson, P.: Spectral interpretation field manual, G-MEX. AusSpec International Pty. Ltd., Unpublished manual (1997).

Price, L., Powell, T.S., and Atkinson, L.: Geothermal fluid evolution at Rotokawa: hydrothermal alteration indicators. Geothermal Resource Council Transactions (2011).

Rae, A.J., O'Brien, J., Ramirez, E., and Bignall, G.: The application of chlorite geothermometry to hydrothermally altered Rotokawa Andesite: Proc. 33rd New Zealand Geothermal Workshop, Auckland, New Zealand, (2011).

Reyes, A.G.: Petrology of Philippine geothermal systems and the application of alteration mineralogy to their assessment. Journal of Volcanology and Geothermal Research 43, pp. 279–309 (1990).

Risk, G.F.: Electrical resistivity of the Rotokawa Geothermal Field: Proc. 22nd New Zealand Geothermal Workshop, Auckland, New Zealand (2000).

Sewell, S.M., Addison, S.J., Hernandez, D., Azwar, L., and Barnes, M.L.: Rotokawa conceptual model update 5 years after commissioning of the 138 MWe NAP Plant. Proc. 37th New Zealand Geothermal Workshop, Taupo, New Zealand (2015).

Simmons, S.F., and Browne, P.R.L.: Hydrothermal minerals and precious metals in the Broadlands-Ohaaki geothermal system: implications for understanding low-sulphidation epithermal environment. Economic Geology 95, pp. 971–999 (2000).

Simpson M.P., and Rae A.J.: Short-wave infrared (SWIR) reflectance spectrometric characterisation of clays from geothermal systems of the Taupō Volcanic Zone, New Zealand. Geothermics 73, pp. 74–90 (2018).

Stimac, J., Moore, J., and Latayan, J.: Hydrothermal alteration and evolution of the Bulalo geothermal field, Philippines. Geothermal Resources Council Transactions, 30, pp. 959–964 (2006).

ISSN 2703-4275

Steiner, A., The Wairakei geothermal area, North Island, New Zealand. New Zealand Geological Survey Bulletin 90, 136 pp (1977).

Tulloch, A.J.: Mineralogical observations on carbonate scaling in geothermal wells at Kawerua and Broadlands. Proc. 4th New Zealand Geothermal Workshop, Auckland, New Zealand (1982).

Wallis, I.C., Bardsley, C.J., Powell, T.S., Rowland, J.V., and O'Brien, J.M.: A structural model for the Rotokawa Geothermal Field, New Zealand. Proc. 35th New Zealand Geothermal Workshop, Rotorua, New Zealand (2013).

Winick, J., Powell, T., and Mroczek, E., The natural-state geochemistry of the Rotokawa reservoir. Proc. 33rd New Zealand Geothermal Workshop, Auckland, New Zealand (2011).

ISSN 2703-4275